Stark broadening of the hydrogen Lyman-α line from the center to the near line wings for low-density plasmas

C. Stehlé
Département d'Astrophysique Fondamentale, Observatoire de Paris—Meudon, 5 place Jules Janssen 92190 Meudon, France
(Received 4 March 1986)

Hydrogen Lyman-α Stark broadening is calculated for a low-density plasma ($N \leq 10^{14}$ cm^{-3}) for detunings smaller than 10 Å in the dipolar and no-quenching approximations. Semiclassical and quantal descriptions are alternatively used to describe the contribution of each collision. The results may be compared with the impact and static approximation limits, thus defining their range of validity and leading to analytical expressions for the relaxation rate in these cases. The effects of the trajectories curvatures and relative velocity variations are analyzed.

I. INTRODUCTION

Recently there has been renewed interest in the Lyman and Balmer lines of hydrogen in low-density plasmas. Some recent laboratory experiments[1] have shown very larger collisional dynamic effects leading to the breakdown of the static theories in the line center. On the other hand, precise computations of the line wings are needed to interpret spectra in experimental conditions where redistribution processes are very large (see for example Basri *et al.*[2] for solar chromosphere spectra). We present here low-density ($N < 10^{14}$ cm^{-3}) Lyman-α calculations from the center to the near line wings.

The impact approximation is valid for electronic and ionic perturbers in the line center, because the collision time is short compared with the atomic dipole relaxation time $\Delta\omega_{1/2}^{-1}$ ($\Delta\omega_{1/2}$ half-width).[3] Moreover, the strong collisions (i.e., which cannot be described by perturbation theory) are separated in time. For large detunings $\Delta\omega$ the typical time of interaction $\Delta\omega^{-1}$ between the collisional complex and the radiation field is small. Thus strong collisions which play a major part in the broadening can be always considered as statistically independent. So if, as pointed out by Smith *et al.*,[4] the impact approximation is valid in the line center, the unified theory can be applied from the center to the wings, leading to the low-density limit of Fano's relaxation theory.[5] The frequency-normalized intensity is then

$$I(\Delta\omega)=\pi^{-1}\mathrm{Im}[\Delta\omega - i\gamma(\Delta\omega)]^{-1} , \quad (1)$$

where the relaxation operator γ varies linearly with N, the density of perturbers.

In the far wings the intensity is attributed to additive independent spontaneous emissions: hence the collisions are very rare events on a time scale of the order of the evolution time $\Delta\omega^{-1}$. After averaging over all the collisions, the intensity varies linearly with the density—this is the one-perturber approximation:[6]

$$I(\Delta\omega)\sim\pi^{-1}\mathrm{Re}[\gamma(\Delta\omega)]/(\Delta\omega)^2 . \quad (2)$$

This approximation, valid in the wings, breaks down in the line center where simultaneous interactions occur during the time of interest $\Delta\omega^{-1}$. In spite of this, the expression obtained for $\mathrm{Re}\gamma(\Delta\omega)$ in the one-perturber theories[7–9] gives the usual impact result $\mathrm{Re}\gamma(0)$ for very small detunings.

Using Fano's expansion of the relaxation operator γ in terms of the collisional perturbation at the low-density limit,[4,5,10] it can be seen that this operator is the Fourier transform of a function equal to zero for negative times (causality principle). The Kramers-Kronig relations are thus satisfied between the real and imaginary parts:

$$\mathrm{Im}\gamma(\Delta\omega)=\frac{1}{\pi}\mathrm{P}\int_{-\infty}^{+\infty}\frac{\mathrm{Re}\gamma(x)}{\Delta\omega - x}dx . \quad (3)$$

The line shape is easily obtained by (1) by calculating the real part and then the imaginary part from (3).

The emission during a collision may be described in either a quantal,[7,11] or a semiclassical formulation.[8,9,12] Except in the case of "satellites" in the wings,[13] these two methods have been only used for the electronic broadening:[14–16] for detunings smaller than 10 Å, the calculations prove that quantum effects (exchange interaction, breakdown of the trajectory notion, etc.) are very small and that the contribution of the polarization and quadrupolar interactions is only 10% of the total intensity beyond 1 Å.[17] For the relatively small detunings involved in the present paper, all these short-range contributions will be neglected. For detunings exceeding 10 Å the large departure from the dipolar approximation requires the use of H^- potential curves.

In the case of H^+ perturbers the unified theory of Vidal *et al.*[18] has been used for the intricate interpretation of solar spectra.[2,19] Other recent calculations have included some dynamics effects at moderate densities[20,21] ($N > 10^{16}$ cm^{-3}) but the earlier studies use the static description for the ionic broadening as a consequence of the large concerned densities.[18,22] Quantum effects are likely to be smaller for protons than for electrons, and adiabatic H_2^+ potentials[23] show that the departures from the dipolar interaction are small for internuclear distances larger than 30 a.u. Assuming, as shown later, that the static approach is valid, the corresponding detuning is ± 10 Å. Thus the discussion will be devoted to the near wing

 ©1986 The American Physical Society

($|\Delta\lambda| < 10$ Å) using dipolar interaction. Doppler broadening, quenching, and fine-structure effects will be neglected. This will be discussed in Sec. IV.

The aim of this paper is to prove that the description of the ionic broadening of the hydrogen lines at low densities differs strongly in the line core where the large dynamics effects lead to the usual impact approximation and in the line wings where the Franck-Condon approach becomes valid, corresponding to the static (Holtsmark in the dipolar approximation) theory. As a consequence of the large perturber mass, the semiclassical approximation for the relative emitter-perturber motion seems justified. This paper will use a quantal approach and a semiclassical one using rectilinear trajectories for the description of the collision. These methods are both particularly attractive because the collisional problem is exactly solved. They have been first introduced by Tran Minh and co-workers,[11] and Lisitsa and Sholin[8] for the calculation of the electronic broadening of the Lyα line wings. The comparison of the results obtained here for the ionic broadening allows us to analyze especially the effects of the trajectories deflection, and of the change of the kinetic energy during the emission.

After a brief review of the methods (Sec. II), the variation of $\mathrm{Re}\gamma(\Delta\omega)$ is analyzed for collisions defined by the same initial kinetic energy but different values of the angular momentum. The intensity is then calculated (Sec. III).

This paper will be concerned mainly with the ionic broadening in a plasma with equal proton and electron densities ($N=10^{13}$ cm^{-3}) at thermodynamical equilibrium ($T=10^4$ K).

II. REVIEW OF THE METHODS

The basic theory has been reviewed in detail by Tran Minh *et al.*[11] and Baryshnikov and Lisitsa[24] and will therefore only briefly be summarized here.

The collisions are defined quantally by the reduced mass m, the initial angular momentum l, and kinetic energy $E=\hbar^2k^2/2m$. In the semiclassical case, the motion is assumed to be described at a constant relative velocity $\mathbf{v}$ on a rectilinear trajectory defined by the impact parameter b. The Coulomb interaction between the emitting dipole and the moving charge can be attributed to a rotating field. Hereafter the initials ($n=2$) and final ($n=1$) states will be denoted, respectively, by Latin and Greek letters.

A. Exact resonance method (ERM)

For hydrogen the collisional problem can be solved "exactly" in the no-quenching approximation because the centrifugal and dipolar potentials both vary in the same way, as r^{-2}.

The constants of the motion are for the upper state the total energy $[E(n=2)+\hbar^2k^2/2m]$, the total angular momentum $\mathbf{L}^T=\boldsymbol{l}+\mathbf{L}$ ($\boldsymbol{l}$ and $\mathbf{L}$ are the orbital and atomic electron angular momenta), and the parity $(-1)^{l+L}$ [and, respectively, $\hbar^2k^2/2m$, $\boldsymbol{\Lambda}^T=\boldsymbol{\lambda}+\boldsymbol{\Lambda}=\boldsymbol{\lambda}$, and $(-1)^{\lambda}$ for the ground state]. The channels are then denoted by (L,l,L^T,M^T) for $n=2$ and by $(\Lambda,\lambda,\Lambda^T,M'^T)$ for the unperturbed ground state ($\Lambda^T=\lambda,\Lambda=0$), corresponding to the radial wave functions $G(r)$. These functions are independent of M^T,M'^T and the isotropic profile also. After a diagonalization of the interaction on this basis, leading to a differential system of equations,[25,26] the radial wave functions (hereafter called the ERM radial wave functions) of the state $n=2$ are the Bessel functions $J_{\mu_m+1/2}(kr)$ corresponding to the diagonal potential energy $(\hbar^2/2m)\mu_m(\mu_m+1)/r^2$ relative to the atomic energy $E(n=2)$. The μ_m values corresponding to a given value of L^T are, respectively,

$$\mu_1=L^T,$$
$$\mu_2=-\tfrac{1}{2}+[(L^T-\tfrac{1}{2})^2-(2L^T+1)(x-1)]^{1/2},$$
$$\mu_3=-\tfrac{1}{2}+[(L^T+\tfrac{3}{2})^2+(2L^T+1)(x-1)]^{1/2},$$

with

$$x=[1+36(m/m_e)^2/(2L^T+1)^2]^{1/2}.$$

These diagonal ERM radial wave functions $J_{\mu_m+1/2}(kr)$ are deduced from the three channels (L_i,l_i,L^T) denoted briefly by i (with $L_1,L_2,L_3=0,1,1$ and $l_1,l_2,l_3=L^T,L^T-1,L^T+1$) by the unitarity transformation $\mathbf{X}$.[11] For the unperturbed ground state, they are simply $J_{\lambda+1/2}(kr)$ corresponding to the centrifugal potential $(\hbar^2/2m)\lambda(\lambda+1)/r^2$.

In the case of weak radiative coupling the transition probability can thus be calculated between all the pairs of exact eigenstates of the collisional complex characterized by (μ_m,λ). This corresponds to the generalized Born (or distorted-wave) approximation for the radiation.[27] Fermi's "golden rule" which gives the radiative transition rate has to be taken between an incoming initial and an outgoing final state for the collisional complex. This seems to disagree with earlier publications[7] considering an incoming wave also for the final state but it can be proved that this has no consequence on the resulting isotropic profile.

The relaxation operator is then given by

$$\gamma(\Delta\omega)=N\int_0^\infty dv_k\, v_k f(v_k)\frac{\pi}{k^2}\times\sum_{L^T=0}^{\infty}(2L^T+1)g(L^T,\Delta\omega,E) \qquad (4)$$

with $\hbar k=mv_k$, $E=(\hbar k)^2/2m$, and

$$\mathrm{Re}g(L^T,\Delta\omega,E)=\frac{\Delta\omega}{6\hbar^2}m^2\delta(\kappa-(k^2-2m\,\Delta\omega/\hbar)^{1/2})\times\sum_{L_{a0}l_{a0}l_i=L^T\mp1,L_i,\Lambda_\alpha,\Lambda^T,\lambda}\left\{\delta(L_i,1)\delta(\Lambda_\alpha,0)\delta(\lambda,l_i)\delta(\Lambda^T,\lambda)\times\left|\int_0^\infty G(L_{a0}kl_{a0}L^T\rightarrow L_ikl_iL^T\,|\,r)G(\Lambda_\alpha\kappa\lambda\Lambda^T\leftarrow\Lambda_\alpha\kappa\lambda\Lambda^T\,|\,r)^*dr\right|^2\right\}. \tag{5}$$

The first Dirac term is a consequence of the total energy conservation (collisional complex and photons). Note also the conservation of the angular momentum for the relative motion $\delta(\lambda,l_i)$.

Overlap integrals in (5) are replaced by convergent integrals of the dipolar interaction matrix elements A_{ij}/r^2 between the channels $i=(L_i,l_i,L^T)$ and $j=(L_j,l_j,L^T)$ giving

$$\mathrm{Re}g(L^T,\Delta\omega,E)=\frac{\pi^2}{6}\sum_{i=2,3}|A_{i1}|^2\sum_{m=1}^{3}[X_{1m}M(\mu_mk,\lambda\kappa)]^2\delta(\lambda,l_i)\,. \tag{6}$$

The overlap integrals M are given by

$$M(\mu_mk,\lambda\kappa)=\int_0^\infty dr\frac{1}{r}J_{\mu_m+1/2}(kr)J_{\lambda+1/2}(\kappa r)\,,$$

and can be expressed in terms of the hypergeometric functions ${}^2F_1$,[28] with different expressions depending on the wing ($k/\kappa\gtrless1$).

B. Semiclassical method (SCM)

For large values of the angular momentum, classical trajectories can be defined by the impact parameter b and velocity $\mathbf{v}$ satisfying the condition

$$L^T\sim l=mvb/\hbar\gg1\,.$$

The potential ERM energies excluding the centrifugal barriers $(\hbar^2/2m)[\mu_i(\mu_i+1)-L^T(L^T+1)]/r^2$ reduce for the state $n=2$ in the three diabatic molecular H_2^+ or H^- potentials $V_1(r)=0$, $V_2(r)=-2lx$, and $V_3(r)=+2lx$ [with $x^2\sim1+9(m/m_e)^2/l^2$]. These potentials can be alternatively obtained for linear trajectories using the semiclassical description of the dipolar interaction in terms of a rotating field $\mathscr{E}(t)$ [with $\mathscr{E}(t)=e/r^2(t)$]. The problem can be solved exactly in a system of coordinates rotating with this perturbating field.[8]

For very large l values the dipolar coupling is small and the trajectories linear. The deflection and change in the relative velocity on the trajectory are negligible according to the inequalities $|V_i(r)|\ll\hbar^2l^2/2mr^2$ or

$$|\mu_i-l|\ll l\,. \tag{7}$$

The emission occurs during the collision, leading to variations of the kinetic energy equal to $\hbar\Delta\omega$ and to modifications of the trajectory. This effect is small at large relative velocities satisfying the condition

$$|\hbar\Delta\omega|/mv^2\ll1\,. \tag{8}$$

When the three preceding inequalities are satisfied, it is easy to prove that the overlap integrals M can be simply expressed in terms of the Bateman functions $k_\nu(y)=W_{\nu/2,1/2}(2y)/\Gamma(1+\nu/2)$ (Whittaker and gamma functions), by

$$M(\mu_mk,l_i\kappa)\sim(\mu_m+l_i+1)^{-1}k_{\mathrm{sgn}(\Delta\omega)\times\nu}(y)\,, \tag{9}$$

with $y=\Delta\omega\,b/v$, and

$$\nu=\mu_m-l_i=\pm1,\pm(1\pm x)\,,\qquad x^2=1+9(m/m_el)^2=1+9(\hbar/m_evb)^2\,. \tag{10}$$

The summation over L^T becomes an integration over b and hence [Eqs. (4) and (5)]

$$\gamma^{\mathrm{sc}}(\Delta\omega)=N\int_0^\infty vf(v)dv\int_0^\infty db\,2\pi bg^{\mathrm{sc}}(b,\Delta\omega,E)\,, \tag{11}$$

with

$$\mathrm{Re}g^{\mathrm{sc}}(b,\Delta\omega,E)=\tfrac{3}{4}\pi^2\left[\frac{m}{m_e}\right]^2\frac{1}{l^2x^2}\left[k_1^2(y)+\frac{9}{2}\left[\frac{m}{m_e}\right]^2\frac{1}{l^2}[k_{1-x}^2(y)+k_{1+x}^2(y)]+[k_\nu(y)\rightarrow k_{-\nu}(y)]\right]. \tag{12}$$

These relations were first given by Lisitsa and Sholin[8] in the formalism of the dipole autocorrelation function and can also be derived by calculating the emission probability of the collisional complex between each pair of diabatic eigenstates.[29] The intensity is the same for $\Delta\omega$ and $-\Delta\omega$ according to the relation $k_\nu(-y)=k_{-\nu}(+y)$. In addition, the relation

$$\mathrm{Re}g^{\mathrm{sc}}(l,\Delta\omega,E)=\mathrm{Re}g^{\mathrm{sc}}(l/q,\Delta\omega\,q,E)\,, \tag{13}$$

valid for any positive value of q, gives a correspondence between the electron and ion contributions taking $q=m_e/m$.

For low l values departures from the rectilinear trajectories and constant velocity assumption lead to an incorrect variation of g^{sc} with l: the effect on the line shape will be analyzed further.

III. VARIATIONS OF γ WITH THE DETUNING

The dynamic relaxation operator $\gamma(\Delta\omega)$ will be calculated from the line center to the near line wings. This requires a precise determination of the hypergeometric and Bateman functions for very large values of the angular momentum leading to some numerical difficulties particularly in the ionic broadening case.

A. Numerical computation

Whittaker functions $W_{\nu,1/2}(x)$ are easily expressed in terms of the Kummer function $U(1-\nu,2,x)$ (Ref. 28), which may be represented by an asymptotic expansion for large x values, by a logarithmic solution for small x values and in general by Chebyshev expansion given by Edmonds and Kelly.[30] They satisfy recurrence relations which can be calculated by the method of continued fractions.[31] For large ν values, the integral representation (p. 405 of Gradshteyn and Ryzhik[32]) has also been used.

The hypergeometric functions ${}^2F_1(a,b,a+b+1,z)$ $(0\leq z\leq 1)$ can be computed by using the limiting expansions for small values of z or $1-z$ and some recurrence relations or their expression in terms of the Whittaker functions (if valid).

In the ERM case the L^T summation is made by a trapezoidal method using a variable step of integration. In expression (6) the contribution of the ERM state corresponding to μ_2 is omitted at low L^T values. Hence for $L^T\leq L^A$ ($L^A=2$ for the electrons, 74 for the protons), the corresponding potential $(\hbar^2/2m)\mu_2(\mu_2+1)/r^2$ is negative in spite of the centrifugal barrier: $\mu_2+\frac{1}{2}$ is thus an imaginary number. In contrast to the repulsive case, the radial wave function oscillates rapidly at small distances. Their overlap $M(\mu_2 k,l_i\kappa)$ with Bessel functions $J_{l_i+1/2}$ of real arguments are neglected for numerical convenience. This point will be justified later.

The lower limit of the energy integration is $E_{inf}=0$ for the red wing or $E_{inf}=\hbar\Delta\omega/kT$ for the blue wing as follows from the Dirac term in expression (5). After the variable E has been transformed to $E-E_{inf}$, a 32-point Gauss-Laguerre integration is used.

In the semiclassical case the g^{sc} functions, (12), are calculated but not the thermal average leading to γ^{sc}, (11). Indeed all the physical conclusions are drawn from the comparison of g with g^{sc}. This comparison and the conclusions of the quantum results for γ will show that an evaluation of the thermal average leading to γ^{sc} is not necessary.

In order to clarify the notation, $\mathrm{Re}\gamma$, $\mathrm{Re}\gamma^{sc}$, $\mathrm{Re}g$, and $\mathrm{Re}g^{sc}$ will be denoted, respectively, by γ, γ^{sc}, g, and g^{sc} (Secs. III A, III B, III C, and III D) except in the case where it becomes necessary to distinguish between the real and imaginary parts (Sec. III E).

B. Line core-impact limit

Near the line center the collision time is negligible in comparison with the time of interest $\Delta\omega^{-1}$. The emission probability varies smoothly along the trajectory[29] and is thus mainly given by contributions from large internuclear distances where the radial wave functions reach their asymptotic forms. The same conclusions can be drawn in the ERM for the overlap integrals which become

$$M(\mu_m k,l_i\kappa)=2\sin[(\mu_m-l_i/2)\pi]/[(l_i+1+\mu_m)(\mu_m-l_i)\pi]\ . \tag{14}$$

The relaxation operator can be expressed in terms of the scattering matrix $\mathbf{S}$:[7,33]

$$g(L^T,0,E)=3^{-1}\sum_{l_i=L^T\mp1}\langle L_i l_i L^T|\,1-\mathbf{S}\,|L_i l_i L^T\rangle\delta(L_i,1)\ . \tag{15}$$

This function is independent of E for a dipolar potential. The semiclassical limit is

$$g^{sc}(l,0,E)=6\left[\frac{m}{m_e}\right]^2\frac{1}{l^2x^2}\left[1+\frac{1+x^2}{1-x^2}\cos^2\left[\pi\frac{x}{2}\right]\right]\ . \tag{16}$$

In the case of heavy perturbers and strong collisions the phase variations in the emission probability along the trajectory[29] lead to oscillations for $g(L^T)$ and $g^{sc}(l)$ about unity. These functions are always lower than $\frac{4}{3}$ because of the unitarity properties of the $\mathbf{S}$ matrix. Trajectory effects appear for the "low" $l\sim L^T$ range excluded by condition (7) and increase for decreasing values of l. As can be seen from (10) the largest values of $|\mu-l|$ for low l values is approximately given by $3(m/m_e)/l$ to be compared with l. Hence for H^+ perturbers these effects are important in the L^T range ($l\sim L^T<70$) where capture into the quasibound state ($\frac{1}{2}+\mu_2$ is an imaginary number, see Sec. III A) may occur for the ERM eigenstate corresponding to μ_2. These effects, hereafter called "short-range effects," cannot be seen with the chosen l scale in Fig. 1 for which the semiclassical and quantal curves are indistinguishable.

For large $l\sim L^T$ values, the SCM and ERM descriptions reduce to the same second-order perturbational expansion:

$$g(l,0,E)\sim 6(m/m_e)^2/l^2=6\hbar^2/m_e^2v^2b^2\leq 1 \quad \text{for } l\geq l_c\ [b\leq b_c(v)]\ . \tag{17}$$

This expression shows the long range of the dipolar interaction, leading to a negligible contribution of the

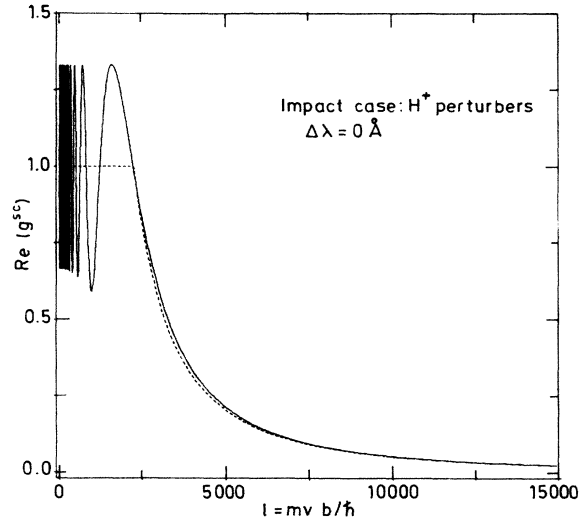

FIG. 1. g^{sc} vs l in the impact case for H^+ perturbers. The dashed line shows the approximate expansion (17) (for $E=1$ eV, $b=0.122l$ a.u.).

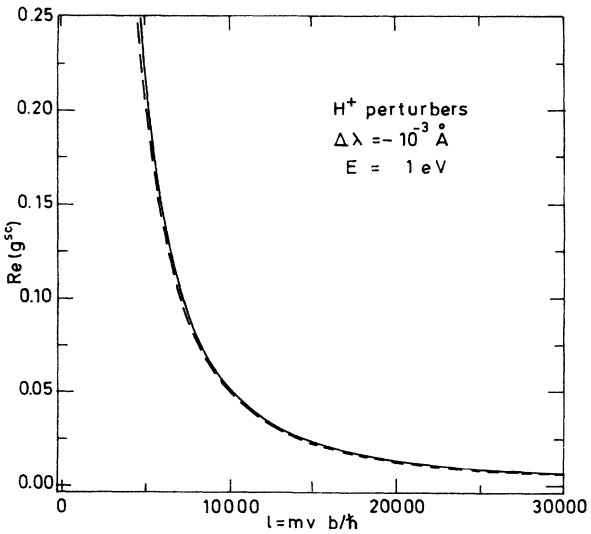

FIG. 3. g^{sc} vs l for the protons near the line center for large l values. The dashed line shows the perturbation impact expression (17).

short-range effects in the relaxation rate $\gamma(0)$. But at large distances it is necessary to introduce the Debye screening effect of the charged perturber bath, by means of $g=0$ for $l \geq l_D = mvb_D/\hbar$.[33] This cutoff, retained for all values of the detuning, is significant only in the line center as will be shown further. Taking $g=1$ for $l \leq l_c = \sqrt{6}m/m_e$ together with the two preceding expressions gives an analytical expression for the average relaxation operator expression, namely,

$$\gamma^{sc}(0)=\gamma(0)=1.566\times 10^{-3}T^{-1/2} \times N[21.12+\ln(T^2/N)] , \quad (18)$$

where the units are rad s^{-1}, K, and cm^{-3}.

In the electronic case the $g^{sc}(l)$ variations are deduced from Fig. 1 after compressing the l scale by the factor m/m_e. Thus $l^c=\sqrt{6}$, and the oscillations, which have been found in earlier publications,[34,35] vanish in the ERM case (Fig. 2). As stated earlier the contribution of the low L^T values leading to capture into a quasibound state is relatively small and the relaxation operator is approximately equal to

$$\gamma(0)\sim\gamma^{sc}(0)=5.168\times 10^{-5}T^{-1/2} \times N[28.64+\ln(T^2/N)] . \quad (19)$$

Expressions (18) and (19) differ slightly from the results of the unified theory,[19] because of different description of the strong collisions contribution and of different Debye values in the ionic case. Hence both the fast electrons and

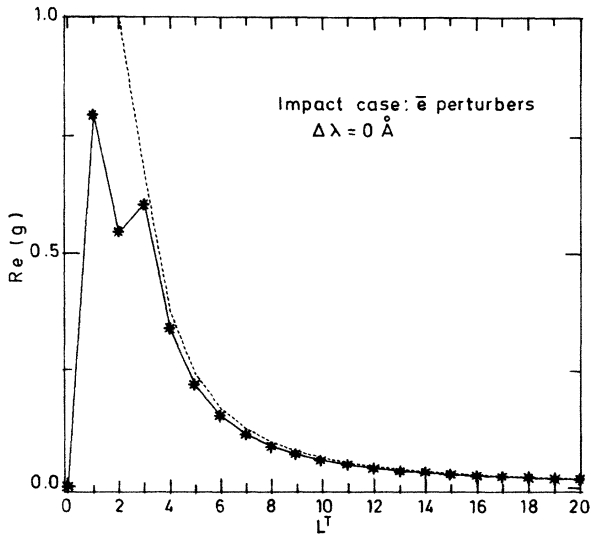

FIG. 2. g vs L^T for the electrons in the impact case. The dashed line shows the approximate expansion (17).

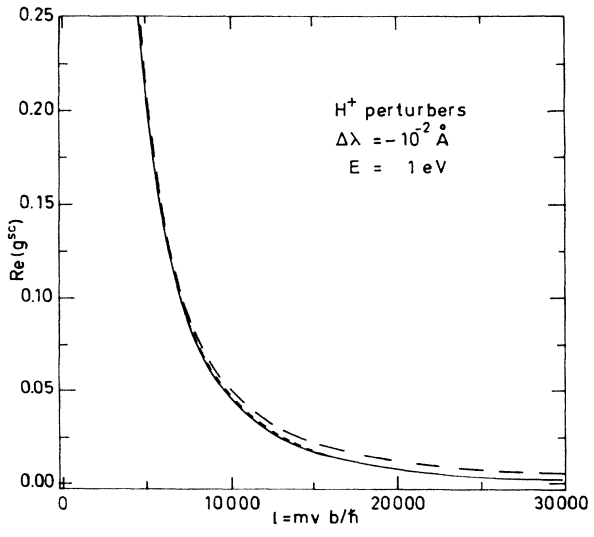

FIG. 4. Same as Fig. 3. The dashed lines show the near impact approximate expansion (20) (- - -) and the impact expression (17) (— — —).

the slow ions contribute to the slow plasma reaction leading to the Debye screening of the ion-hydrogen interaction.[33]

To ensure that the impact approximation is valid up to the half-width, the condition $\Delta\omega_{1/2}b/v \ll 1$ has to be satisfied even at large distances. By taking the Debye radius for b and the mean velocity for v this gives $N \leq 10^{14}$ cm^{-3} at 10^4 K for the ionic broadening.

As mentioned in the Introduction, the strong collisions [$b \leq b_c(v)$ or $l \leq l_c$] do not overlap in time. The required condition $4.84\times10^{-16}(m/m_e)NT^{-3/2} \ll 1$ is satisfied in this density range.

C. Near line wings

Near impact region. Departures from the impact approximation for a collision (v,b) are specified by the magnitude of the quantity $y\nu=\nu\Delta\omega b/v$, where ν [Eq. (10)] is a measure of the strength of the collisional interaction. This can be shown in the semiclassical formulation by expanding $[k_\nu^2(y)+k_{-\nu}^2(y)]$ to the first order in y.

For large b values ($|\nu| \sim 1$) the impact approach breaks down for detunings satisfying $\Delta\omega b_D/v \geq 1$ corresponding to $|\Delta\lambda| \geq 10^{-3}$ Å (10^{-2} Å for electrons). In the case of the strong collisions (small b values) the same condition $|y\nu| \geq 1$ is valid until $|\Delta\lambda| \geq 10^{-2}$ Å (1 Å for the electrons) so that, for $10^{-3} < \Delta\lambda < 10^{-2}$ Å, the impact approximation can be used for strong collisions, but not for the weak ones, leading to the following approximate form for g^{sc}:

$$g^{sc}(l,\Delta\omega,E)=1 \quad \text{for } l \leq l_c \ ,$$
$$g^{sc}(l,\Delta\omega,E)=6(m/m_e)^2A(y)/l^2 \quad \text{for } l_c \leq l \leq l_D \ , \tag{20}$$

where $A(y)=y^2[K_1^2(|y|)+K_0^2(|y|)]=(\pi^2/8)[k_1^2(y)+k_{-1}^2(y)]$ and corresponds to the second-order expansion in the collisional perturbation of the relaxation theory[5]

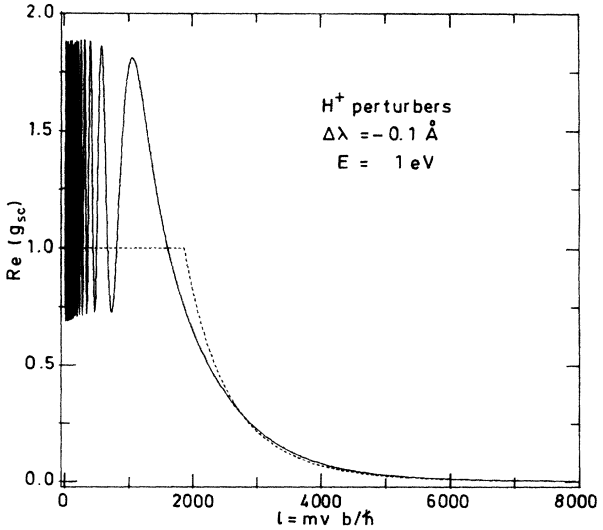

FIG. 5. g^{sc} vs l in the intermediate region. The dashed line shows the near impact approximation (20).

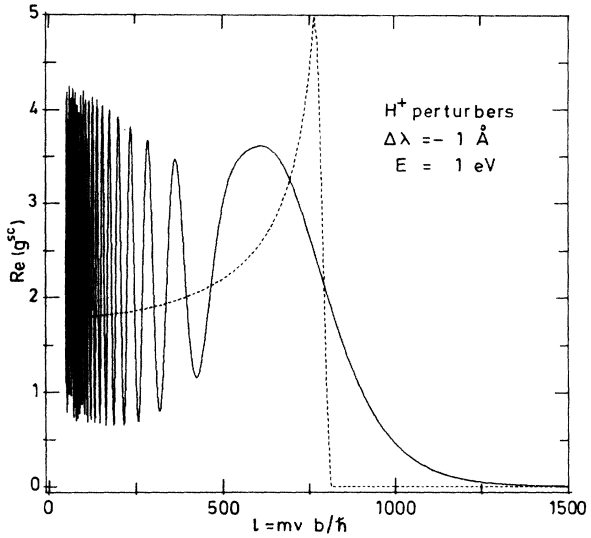

FIG. 6. g^{sc} vs l for a large detuning. The dashed line shows the mean value of the l oscillations given by the result of the stationary phase method [Eqs. (22) and (23)].

(K_0 and K_1 are the usual modified Bessel functions). This function has been used for the impact broadening of isolated lines.[36] Figures 3 and 4 give the variation of g^{sc} with b (expressed in units of $\hbar/mv$). It can be seen that the exact and approximate near impact results are indistinguishable and differ from the impact curve only at large b values. Short-range effects are also negligible as in Sec. III A and the ERM results have not been plotted.

Intermediate region. For increasing detunings we can use the asymptotic expansion for the Bateman function [$k_\nu(|y|)$ not too large]:

$$k_\nu^2(|y|)=k_{-\nu}^2(-|y|)\sim\exp(-2|y|)\frac{|2y|^\nu}{\Gamma(1+\nu/2)^2} \ ,$$
$$|y| \gg 1 \ . \tag{21}$$

Hence the contribution of large-distance interactions vanishes as $\exp[-2b/b_\omega(v)]$, where $b_\omega(v)=|v/\Delta\omega|$ is the usual Lewis[37] cutoff. The Debye screening becomes ineffective as soon as the Debye radius is much larger than b_ω ($\Delta\omega b_D/v \gg 1$). At 0.1 Å, for example, and $E=1$ eV, we have $b_\omega=300$ a.u. and $b_D=3\times10^4$ a.u., corresponding, respectively, to $l_\omega \sim 3\times10^4$ and $l_D \sim 3\times10^6$.

The $g(l)$ function is no longer connected with the **S** matrices for the strong collisions because the impact theory breaks down and the mean value of the oscillations is enhanced for increasing detunings (Fig. 5).

In this intermediate region ($|\Delta\lambda| < 1$ Å), the velocity variations after the emission are rather small [condition (8)]. Short-range effects are negligible after the average leading to γ (γ^{sc}). ERM and SCM curves are indistinguishable.

D. Large detunings

Beyond 1 Å, the small angular momentum contribution becomes larger (Figs. 6 and 7) and the Bateman function

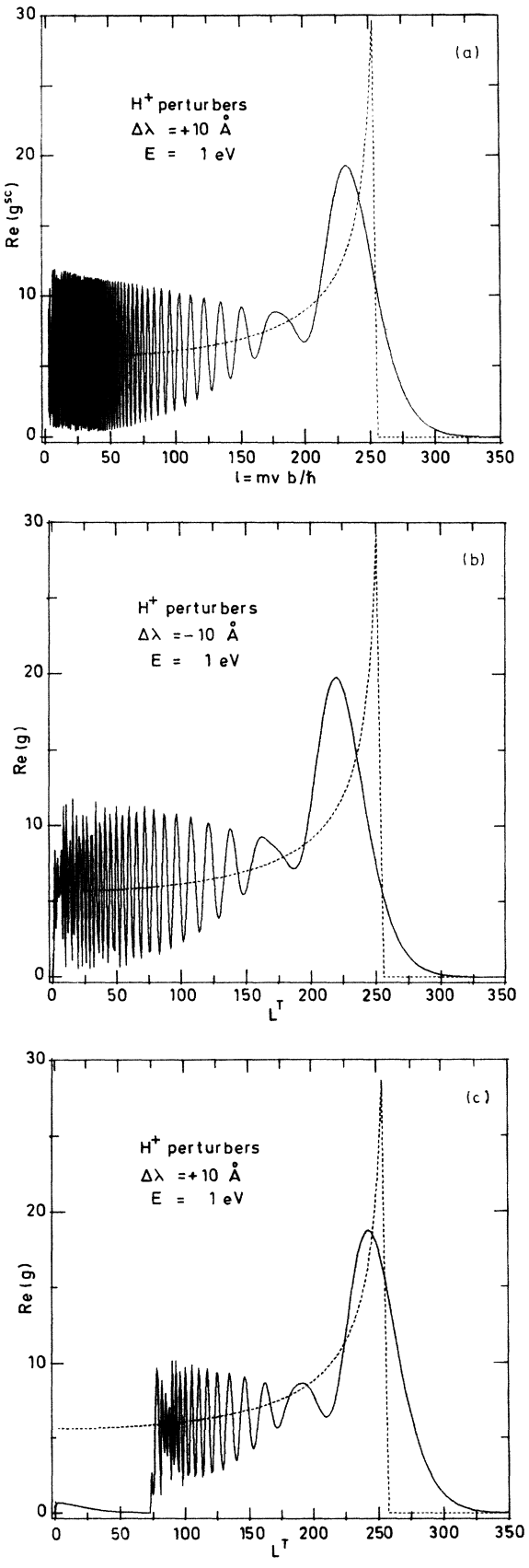

FIG. 7. (a) Same as Fig. 6. (b) and (c) Same as Fig. 6 but relative to the variations of g vs L^T.

is negligible for moderate values of $|\nu|$ [Eq. (21)]. Expression (12) becomes

$$g^{sc}(l,\Delta\omega,E)\sim\frac{27\pi^2}{4}\left[\frac{m}{m_e}\right]^4\frac{1}{l^4x^2}k^2_{3(m/m_e)(1/l)}(|y|)\,. \tag{22}$$

The emission occurs mainly at the Franck-Condon point R_0 (Ref. 29) defined by $|\Delta\omega|=3\hbar/m_eR_0^2$. The detuning is here equal to the shift induced by the electrostatic field created by the charged perturber at the distance R_0. The stationary phase or saddle-point method can be used to calculate the Bateman function:[38]

$$k_\nu(y)^2\sim\frac{4}{\pi\nu\tan\phi_0}\sin^2\left[\frac{\pi}{4}+\nu\phi_0-\frac{\nu}{2}\sin(2\phi_0)\right] \tag{23}$$

with $\phi_0=\arccos(b/R_0)$ and $\nu,y>0$. At large l (or b) values ($b\geq b_s=3\hbar/m_e|\Delta\omega|$) there is a strong decrease of g^{sc} corresponding to the classically forbidden region ($R_0\leq b$) [Fig. 7(a)]. The strong oscillations of $\sin^2$ in expression (23), related to the phase of the wave function at the Franck-Condon point,[29] can be weighted to $\frac{1}{2}$. After averaging b from 0 to b_s, expressions (11), (22), and (23) yield the usual quasistatic Holtsmark result:

$$\gamma^{sc}(|\Delta\omega|)=\sqrt{3}\pi N(\hbar/m_e)^{3/2}|\Delta\omega|^{-1/2}\,. \tag{24}$$

Validity conditions of this derivation are discussed elsewhere.[29] The condition $|3\hbar\Delta\omega/m_ev^2|>\pi^2$ gives the validity range $|\Delta\lambda|>1$ Å for the Holtsmark approximation for H^+ perturbers. In the electronic case, the required detuning ($|\Delta\lambda|>100$ Å) is incompatible with the dipolar approximation and the use of the classical trajectories.

Trajectory effects appear for the low $l\sim L^T$ range excluded by condition (7) [i.e., $|\mu-l|\sim 3(m/m_e)/l\ll l$]. For the large detunings involved here, they are responsible for some discrepancies between the variations of g and g^{sc} with l. In particular the quantal curves are slightly different depending on the sign of the detuning (Fig. 7) contrary to the semiclassical case. For the ERM case the "Franck-Condon points" R_0 (if any) must satisfy one of the six relations ($m=1,2,3$ and $l_i=L^T\pm1$)

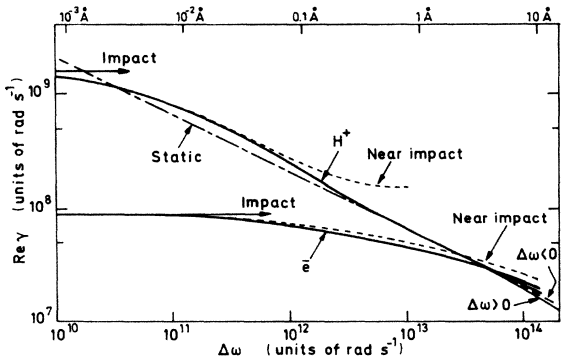

FIG. 8. H^+ and electron contributions to $\mathrm{Re}\gamma(\Delta\omega)$ vs $\Delta\omega$ with the impact, near impact, and static limits ($N=10^{13}$ cm^{-3}, $T=10^4$ K). Units are rad s^{-1} for $\Delta\omega$ and γ.

$$\hbar\Delta\omega=(\hbar^2/2m)[\mu_m(\mu_m+1)-l_i(l_i+1)]/R_0^2 .$$

The right member of this equation corresponds to the potential difference between the collisional ERM eigenstates before and after the emission. For a positive (negative) detuning the solution R_0 exists only for the eigenstate denoted by $m=3$ ($m=2$). The value of this "quantal Franck-Condon point" is near its classical value. However, the oscillations of g with L^T are more rapid for the red wing than for the blue ones contrary to the semiclassical case. This can be attributed to different trajectory curvatures and relative velocity variations on these trajectories. But the mean value of these oscillations is in good agreement with the result of the saddle-point method [expressions (22) and (23) taking $\sin^2=\frac{1}{2}$] as can be seen from Figs. 7(b) and 7(c).

This proves that these trajectory effects are negligible after L^T summation (4). However, in the quantal case, the omission, for numerical convenience, of the μ_2 contribution leading to capture into quasibound states ($L_T<74$) slightly underestimates the total red wing intensity. The result of the saddle-point method seems to give a good estimation of this neglected contribution [Fig. 7(c)], giving after energy integration a total intensity close to the Holtsmark result. This point will be shown in the next section.

E. Line shape

The real part of the dynamic relaxation operator $\gamma(\Delta\omega)$ is calculated by mean of expression (4). ERM results are compared for electrons and protons with the impact [Eqs. (18) and (19)], near impact [Eq. (20)], and static [Eq. (24)] limiting cases in Fig. 8. It can be shown that the first and second approximations are convenient in the H^+ case in the detuning ranges $0-10^{-3}$ Å and $10^{-3}-10^{-2}$ Å, respectively. The Holtsmark formulation is appropriate beyond 1 Å for the red wing but the neglect of the contributions

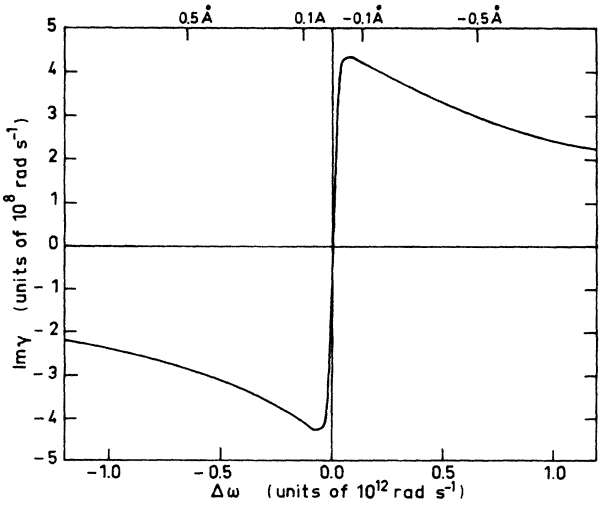

FIG. 9. $\mathrm{Im}\gamma(\Delta\omega)$ as a function of $\Delta\omega$ for the protons. Units are 10^{12} rad s^{-1} for $\Delta\omega$ and 10^8 rad s^{-1} for $\mathrm{Im}\gamma(\Delta\omega)$. ($N=10^{13}$ cm^{-3}, $T=10^4$ K.)

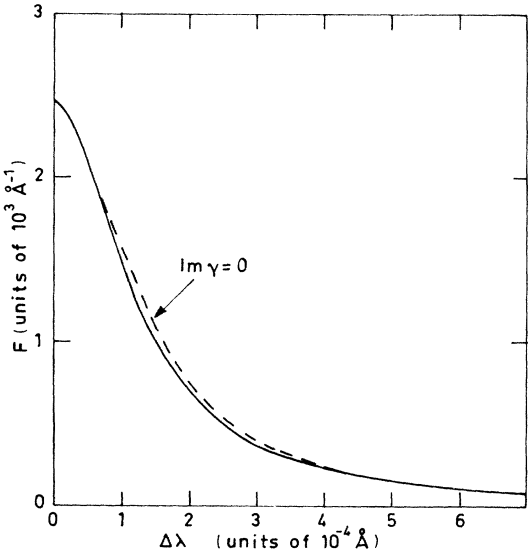

FIG. 10. Wavelength-normalized total intensity $F(\Delta\lambda)$ vs $\Delta\lambda$ (electrons and ions) at 10^{13} cm^{-3} and 10^4 K. The dashed line shows the result without dynamic shift ($\mathrm{Im}\gamma=0$). Units are 10^3 Å^{-1} for F and 10^{-4} Å for $\Delta\lambda$.

leading to capture into a quasibound state is responsible for a little underestimation of the intensity for detunings larger than 5 Å. The energy threshold value $\hbar\Delta\omega/kT$ for positive detunings $\Delta\omega$ gives rise to a lower intensity for the blue wing if the condition $\hbar\Delta\omega/kT\geq 0.05$ is satisfied (i.e., $\Delta\lambda\leq -5$ Å). The relaxation operator is then, in the static approximation, obtained from the Holtsmark result (24) after multiplication by the Boltzman factor $\exp[-(\hbar\Delta\omega/kT)]$.[39]

With regard to the electronic broadening, the impact approach can be used in the range $0-10^{-2}$ Å, and the near impact between 10^{-2} and 1 Å. The static regime is not reached. All these results agree with the preceding discussion. They also prove that the semiclassical approach of Lisitsa and Sholin[8] would give very accurate results.

In the line center the line shift $\mathrm{Im}\gamma(0)$ is related to the wings asymmetry as can be shown by the Kramers-Kronig relation. As this asymmetry effect becomes visible in the static region an approximate expression is given by $\mathrm{Im}\gamma(0)\sim -6.63\times 10^{-5}NT^{-1/2}$ (5×10^{-7} Å at 10^4 K and 10^{13} cm^{-3}). Relation (3), giving $\mathrm{Im}\gamma(\Delta\omega)$ as a function of $\mathrm{Re}\gamma$, can be expressed in terms of the difference $[\mathrm{Re}\gamma(\Delta\omega+x)-\mathrm{Re}\gamma(\Delta\omega-x)]$ on both sides of the considered detuning. So, near the line center, very accurate results would be necessary for $\mathrm{Re}\gamma$ which varies very slowly with the detuning.

The shift contribution can be neglected as long as $|\mathrm{Im}\gamma|$ is much smaller than the detuning. This is always the case for the electrons and for detunings larger than 10^{-3} Å for the protons as well. Near the line center, the computation of the H^+ dynamic shift (see Fig. 9)., which needs a smoothing of $\mathrm{Re}\gamma(\Delta\omega)$, is not very accurate. But its effect is relatively small in this profile region where the Doppler broadening is very large (Fig. 10). Thus $\mathrm{Im}\gamma(\Delta\omega)$ can be set equal to zero from the line center to the wings and the one perturber approximation becomes

valid as soon as $|\mathrm{Re}\gamma(\Delta\omega)|$ is negligible compared with $|\Delta\omega|$ [$|\Delta\lambda| > 0.1$ Å].

The electronic contribution to the intensity is very small in the near line wings. Hence the dynamic effects enhance the relative contribution of the heavy perturbers [Eqs. (18) and (19)]. It becomes on the same order of magnitude as the H^+ contribution towards 1 Å.

IV. DISCUSSION AND CONCLUSION

These results show that the trajectory effects (departure from the assumption of rectilinear trajectory and constant relative velocity) are very small after the collisional average [Eqs. (4) and (11)] for the protons and electrons in the relevant density range. But the energy variation during the emission leads to a small asymmetry which cannot be treated by the semiclassical description of Lisitsa an Sholin.[8]

Concerning the ERM, the omission at small L^T values of the eigenstate contribution corresponding to imaginary values of $(\mu_2+\frac{1}{2})$ is negligible in the line center, but slightly underestimates the intensity beyond 1 Å in the blue wing only. In the case of the electronic broadening, the resulting error is very small for detunings smaller than 10 Å. This can be shown by the comparison of the results of the present ERM method ($T=12\,200$ K) (see Fig. 11) with the calculations of Feautrier *et al.*,[14] and Feautrier and Tran-Minh[40] which include these capture effects and other short-range interactions for $L^T \leq 2$.

The method is valid as long as the impact theory is adequate at the line center ($N \leq 10^{14}$ cm^{-3}). The calculated values for $\mathrm{Re}\gamma(\Delta\omega)$ can be used, at the same temperature, at other densities, provided that $\mathrm{Re}\gamma(\Delta\omega)$ varies linearly with the density. This requires that $\Delta\omega\, b_D/v > 1$, as discussed in Sec. III B. Hence the present results can be used at densities lower than 10^{13} cm^{-3} for detunings larger than 10^{-2} Å for the electrons and 10^{-3} Å for the protons. At smaller detunings expressions (18), (19), and (20) may be used.

At low densities the collisional duration is small in comparison with the time between two collisions according to the condition $\Delta\omega_{1/2} b_D/v < 1$. Between two collisions, spontaneous emission occurs for the hydrogen atom leading to the usual relaxation rate $\gamma_{es} = A/2 = 3.13\times10^8$ rad s^{-1} which adds to $\gamma(\Delta\omega)$.

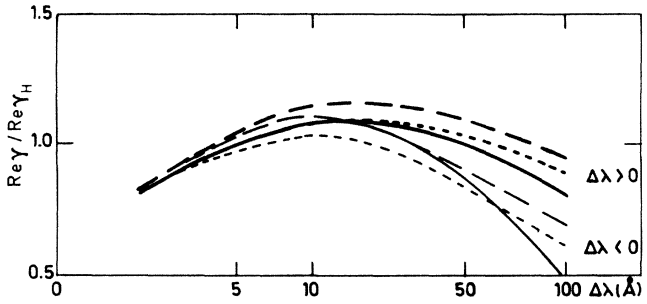

FIG. 11. Reγ normalized to the Holtsmark result (24) as a function of the detuning $\Delta\lambda$ (Å) for the electrons ($N=8.4\times10^{16}$ cm^{-3}, $T=12\,200$ K) compared with the results of Feautrier *et al.* (Ref. 14) (dashed line) and Feautrier and Tran Minh (Ref. 40) (dotted line), for the red and blue wings.

Spontaneous emission effects and spin-orbit interaction are responsible for the splitting of the energy levels. The Lyα line has to components separated by 5.4×10^{-3} Å corresponding to the transitions $2p_{3/2}\rightarrow 1s_{1/2}$ and $2p_{1/2}\rightarrow 1s_{1/2}$. In the line center it can be shown[41] that the large contribution of the long-range interactions allows us to use a perturbational description of the collision, coupling principally the states $2p_{3/2}$ and $2p_{1/2}$ to the state $2s_{1/2}$. Thus the energy splitting effects can be neglected for the densities satisfying the condition $|\Delta\omega_{2s_{1/2}\text{-}2p_{3/2}} b_D/v| < 1$. The required large densities ($N > 10^{15}$ cm^{-3}) violate the condition for the impact approximation to be valid. In the line wings however this effect vanishes for detunings larger than all the energy separations in $n=2$ (i.e., $|\Delta\lambda| \gg 5\times10^{-3}$ Å).

The resulting profile has finally to be convolved with the Doppler broadening ($\Delta\lambda_{1/2D} \sim 4\times10^{-3}$ Å at 10^4 K), whose influence is negligible for $|\Delta\lambda| > 1$ Å because of its exponential decrease.

ACKNOWLEDGMENTS

I would like to thank Dr. N. Feautrier for suggesting this research and Dr. J. Dubau for helpful discussions. The calculations have been done at the Centre Inter-Régional de Calcul Electronique (BP63-91406 ORSAY-CEDEX) on a NAS9080 computer.

[1]E. W. Weber, R. Frankenberger, and M. Schilling, Appl. Phys. B 32, 63 (1983).
[2]G. S. Basri, J. L. Linsky, J. D. F. Bartoe, G. Brueckner, and M. E. Van Hoosier, Astrophys. J. 230, 924 (1979).
[3]C. Stehlé, A. Mazure, G. Nollez, and N. Feautrier, Astron. Astrophys. 127, 263 (1983).
[4]E. W. Smith, C. F. Hooper, and L. J. Roszman, J. Quant. Spectrosc. Radiat. Transfer 13, 1523 (1973).
[5]U. Fano, Phys. Rev. 131, 259 (1963).
[6]M. Baranger, in *Atomic and Molecular Processes*, edited by D. R. Bates (Academic, New York, 1962).
[7]N. Tran Minh and H. Van Regemorter, J. Phys. B 5, 903 (1972).
[8]V. S. Lisitsa and G. V. Sholin, Zh. Eksp. Teor. Fiz. 61, 921 (1971) [Sov. Phys.—JETP 34, 484 (1972)].
[9]H. Pfenning, J. Quant. Spectrosc. Radiat. Transfer 12, 821 (1972).
[10]E. W. Smith and C. F. Hooper, Phys. Rev. 157, 126 (1967).
[11]N. Tran Minh, N. Feautrier, and H. Van Regemoter, J. Quant. Spectrosc. Radiat. Transfer 16, 849 (1976).
[12]L. Spitzer, Phys. Rev. 58, 348 (1940).
[13]Le Quang Rang and D. Voslamber, J. Quant. Spectrosc. Radiat. Transfer 25, 35 (1981).
[14]N. Feautrier, N. Tran Minh, and H. Van Regemorter, J. Phys.

B 9, 1871 (1971).
[15]M. Caby-Eyraud, G. Coulaud, and Nguyen Hoe, J. Quant. Spectrosc. Radiat. Transfer **15**, 593 (1975).
[16]D. Voslamber, Phys. Lett. **61A**, 27 (1977).
[17]N. Tran Minh, N. Feautrier, and A. R. Edmonds, J. Quant. Spectrosc. Radiat. Transfer **23**, 377 (1980).
[18]C. R. Vidal, J. Cooper, and E. W. Smith, J. Quant. Spectrosc. Radiat. Transfer **10**, 1011 (1970).
[19]J. B. Yelnik, K. Burnett, J. Cooper, R. J. Ballagh, and D. Voslamber, Astrophys. J. **248**, 705 (1981).
[20]R. W. Lee, J. Phys. B **12**, 1145 (1979).
[21]R. L. Greene, J. Quant. Spectrosc. Radiat. Transfer **27**, 639 (1982).
[22]H. R. Griem, Phys. Rev. **140**, 1140 (1965).
[23]M. Madsen and J. M. Peek, At. Data **2**, 171 (1971).
[24]F. F. Baryshnikov and V. S. Lisitsa, Zh. Eksp. Teor. Fiz. **72**, 1797 (1977) [Sov. Phys.—JETP **45**, 943 (1977)].
[25]I. C. Percival and M. J. Seaton, Proc. Cambridge Philos. Soc. **53**, 654 (1957).
[26]M. J. Seaton, Proc. Phys. Soc. London **77**, 174 (1961).
[27]A. Messiah, *Mécanique Quantique* (Dunod, Paris, 1959).
[28]*Handbook of Mathematical Functions,* edited by M. Abramowitz and I. A. Stegun (Dover, New York, 1972).
[29]C. Stehlé and N. Feautrier, J. Phys. (Paris) **47**, 1015 (1986); Ann. Phys. (Paris) Colloq. No. 3, Suppl. No. 3, **11** (1986).
[30]A. E. Edmonds and B. A. Kelly (private communication).
[31]H. F. Arnoldus, Comput. Phys. Commun. **33**, 347 (1984).
[32]*Table of Integrals, Series and Products,* edited by I. S. Gradshteyn and I. M. Ryzhik (Academic, New York, 1965).
[33]C. Stehlé and N. Feautrier, J. Phys. B **17**, 1477 (1984).
[34]M. E. Bacon, K. Y. Shen, and J. Cooper, Phys. Rev. **188**, 50 (1969).
[35]K. Y. Shen and J. Cooper, Astrophys. J. **155**, 37 (1969).
[36]H. R. Griem, M. Baranger, A. C. Kolb, and G. Oertel, Phys. Rev. **125**, 177 (1962).
[37]M. Lewis, Phys. Rev. **121**, 501 (1960).
[38]H. Buchholz, *The Confluence Hypergeometric Function* (Springer, Berlin, 1969).
[39]K. M. Sando and P. S. Herman, in *Spectral Line Shapes,* edited by K. Burnett (de Gruyter, Berlin, 1983).
[40]N. Feautrier and N. Tran-Minh, J. Phys. B **10**, 3427 (1977).
[41]C. Stehlé and N. Feautrier, J. Phys. B **18**, 1297 (1985).

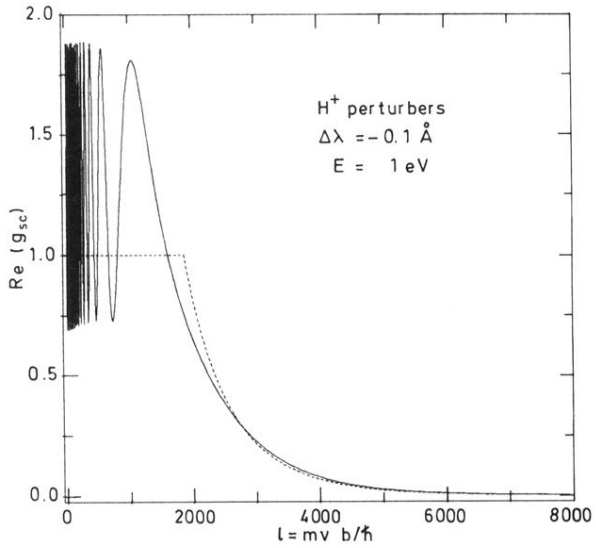

FIG. 5. g^{sc} vs l in the intermediate region. The dashed line shows the near impact approximation (20).

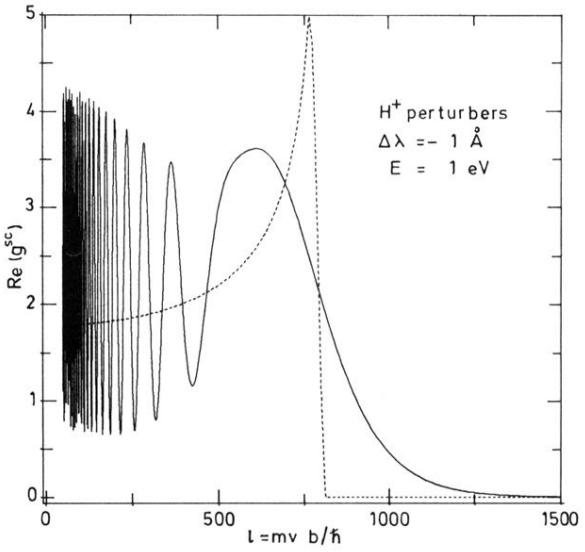

FIG. 6. g^{sc} vs l for a large detuning. The dashed line shows the mean value of the l oscillations given by the result of the stationary phase method [Eqs. (22) and (23)].

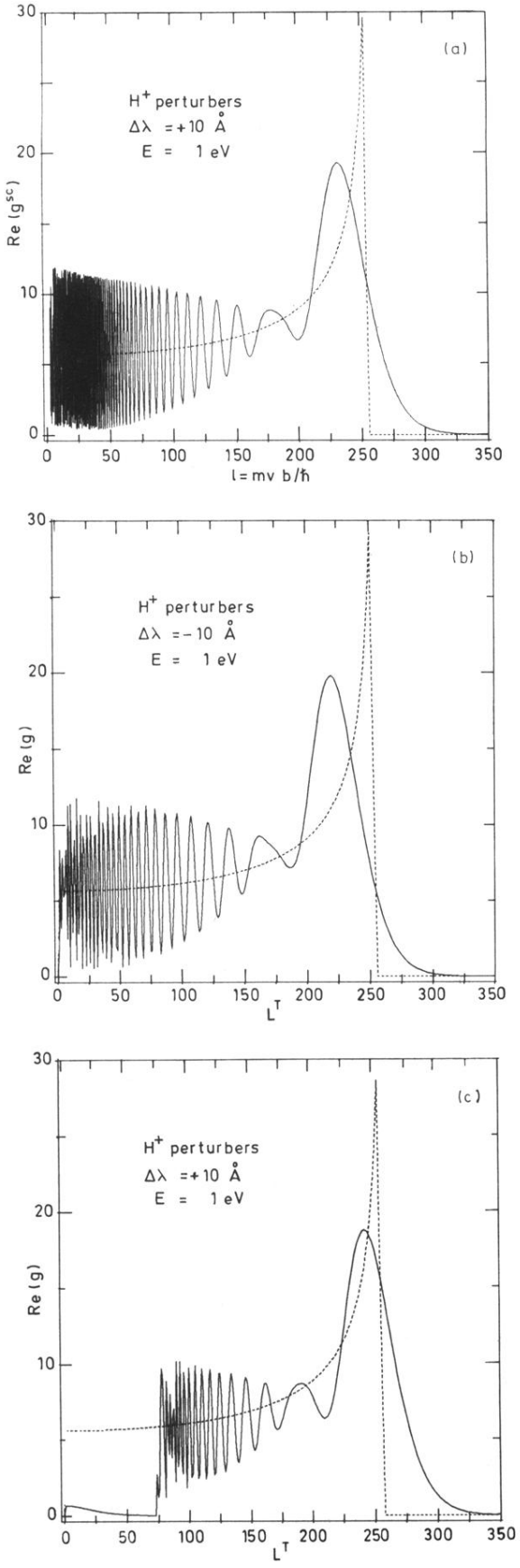

FIG. 7. (a) Same as Fig. 6. (b) and (c) Same as Fig. 6 but relative to the variations of g vs L^T.